# HIGHLIGHTS FROM THE PHENIX EXPERIMENT*

Sanghoon Lim

for the PHENIX Collaboration

Pusan National University, South Korea

*Received 1 August 2022, accepted 15 September 2022,*
*published online 14 December 2022*

PHENIX has performed an extensive study on the evolution of medium effects from small to large systems. PHENIX has continued searching for Quark–Gluon Plasma (QGP) in small systems by measuring collectivity, modification of light hadron and quarkonia production, and jet substructure. In large systems, detailed studies on the property of the QGP have been done using direct photon, $\pi^0$-hadron correlation, heavy-flavor electron, and $J/\psi$ flow with large statistics of data collected in 2014. This report covers new results from the PHENIX experiment in various collision systems.

DOI:10.5506/APhysPolBSupp.16.1-A7

## 1. Searching for QGP in small systems

### *1.1. Collectivity*

PHENIX previously published results of elliptic and triangular flow in 0–5% $p/d/^3$He+Au collisions at $\sqrt{s_{NN}} = 200$ GeV [1]. The results show a strong relation between initial geometry and flow which is evidence of QGP droplet in small systems. A new analysis has been performed using three combinations of two-particle correlations [2]. Figure 1 shows elliptic and triangular flow of charged particles as a function of $p_{\mathrm{T}}$ in 0–5% $p/d/^3$He+Au collisions using two different methods. The new results with the $3 \times 2$PC method are consistent with the previous results with the event-plane method. More detailed studies are done to extract flow coefficients at various kinematic regions, and such a study can help to understand the origin of azimuthal anisotropies such as flow, nonflow, and longitudinal decorrelation in different kinematic regions [2, 3].

* Presented at the 29$^{\text{th}}$ International Conference on Ultrarelativistic Nucleus–Nucleus Collisions: Quark Matter 2022, Kraków, Poland, 4–10 April, 2022.

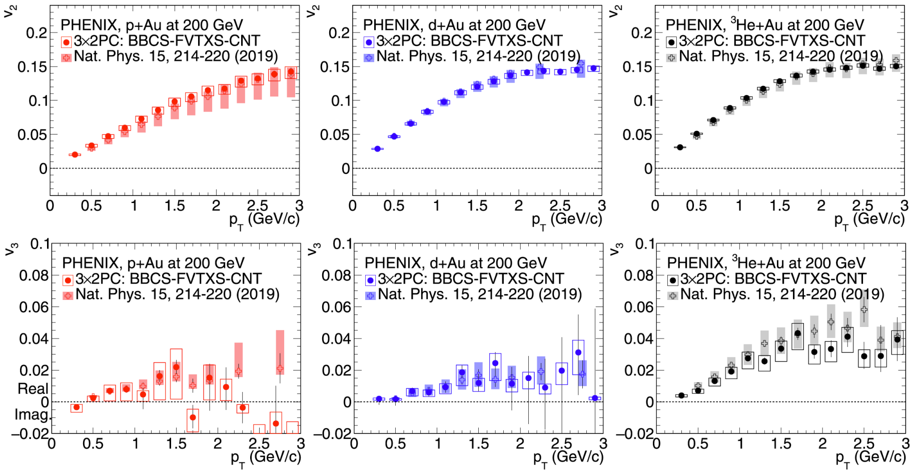


Fig. 1. Elliptic (top) and triangular (bottom) flow of charged particles as a function of $p_{\mathrm{T}}$ at mid-rapidity in 0–5% $p/d/^{3}$He+Au collisions at $\sqrt{s_{NN}} = 200$ GeV.

### 1.2. Nuclear modification of light-flavor hadrons

A study of production of light-flavor hadrons in various centrality ranges of small collision systems can provide detailed information on the evolution of initial-state and final-state effects. Figure 2 shows the nuclear modification factor of $\pi^0$ and $\phi$ as a function of $p_{\mathrm{T}}$ in central and peripheral collisions [4, 5]. In central collisions, there is a $p_{\mathrm{T}}$ broadening in $2 < p_{\mathrm{T}} < 6$ GeV/$c$, and it is more pronounced in $p$+Au collisions compared to $p$+Al collisions of a

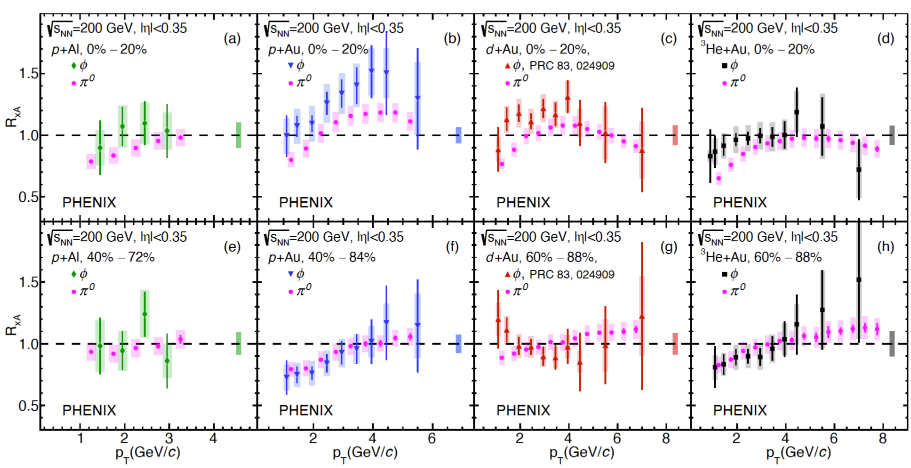


Fig. 2. Nuclear modification factor of $\phi$ and $\pi^0$ as a function of $p_{\mathrm{T}}$ in central (top) and peripheral (bottom) collisions of small systems at $\sqrt{s_{NN}} = 200$ GeV.

different target and $^3$He+Au collisions of a different projectile. The radial flow could explain this $p_T$ broadening. In the comparison between $\pi^0$ and $\phi$, the nuclear modification factor of $\phi$ is slightly above $\pi^0$ in central collisions. This indicates a multiplicity-dependent strangeness enhancement in small systems.

One interesting observation in the nuclear modification factor of $\pi^0$ at high $p_T$ is a suppression (enhancement) in central (peripheral) collisions. To investigate the origin of the modification, PHENIX has measured the nuclear modification factor of $\pi^0$ and direct $\gamma$ at high $p_T$ in various centrality of $d$+Au collisions at $\sqrt{s_{NN}} = 200$ GeV. A similar enhancement is observed in the nuclear modification factor of direct $\gamma$ in peripheral collisions, but there is no suppression in central collisions. To eliminate a possible bias from the centrality selection and $\langle N_{\text{coll}} \rangle$ calculation, the ratio of nuclear modification factors between $\pi^0$ and direct $\gamma$ is calculated as shown in the left panel of Fig. 3. The right panel shows the quantity as a function of charged particle multiplicity. In high multiplicity $d$+Au collisions, there is a clear indication of nuclear effects suppressing $\pi^0$ production.

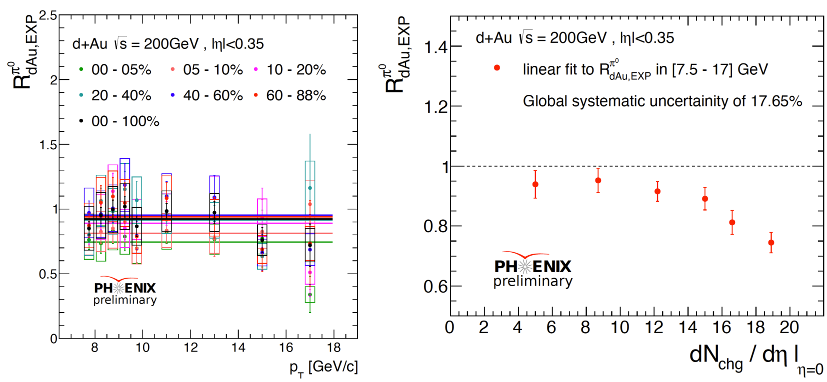


Fig. 3. Nuclear modification factor of $\pi^0$ with respect to the nuclear modification of direct $\gamma$ at high $p_T$ in various centrality of $d$+Au collisions at $\sqrt{s_{NN}} = 200$ GeV.

### *1.3. Charmonia production*

PHENIX previously published the nuclear modification of inclusive $J/\psi$ in various small collision systems [6]. The suppression of $J/\psi$ at the backward rapidity (Au-direction), which nuclear parton distribution functions (nPDFs) could not explain, suggests the final-state effects on the $J/\psi$ production. A new analysis has been done to measure the nuclear modification factor of $\psi(2S)$ which could provide additional information on the final-state effects compared with the $J/\psi$ results. This is because it is expected that the initial-state effects on $J/\psi$ and $\psi(2S)$ production are similar. Figure 4 shows the nuclear modification factor of $J/\psi$ and $\psi(2S)$ at backward (left) and forward (right) rapidity as a function of centrality in $p$+Au collisions at $\sqrt{s_{NN}} = 200$ GeV [7]. The modification of $J/\psi$ and $\psi(2S)$ is similar at forward rapidity which can be explained by models including nPDFs. At backward rapidity, $\psi(2S)$ is more strongly suppressed than $J/\psi$ in central collisions. The transport model considering the final-state effects can describe the data qualitatively.

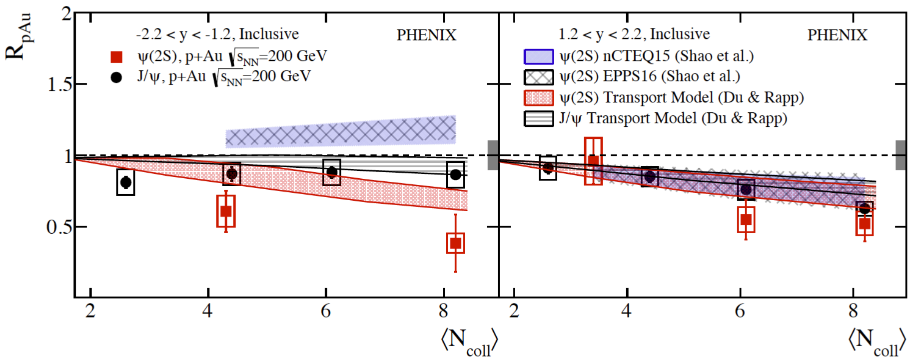


Fig. 4. Nuclear modification of $J/\psi$ and $\psi(2S)$ at backward (left, Au-direction) and forward (right, $p$-direction) rapidity as a function of $\langle N_{\rm coll}\rangle$ in $p$+Au collisions at $\sqrt{s_{NN}} = 200$ GeV.

## 2. Detailed study on QGP in large systems

### *2.1. Direct photon*

Direct photons are important probes to understand the evolution of the medium produced in heavy-ion collisions. PHENIX previously showed that the yields of direct photons at a low $p_{\rm T}$-scale with the charged particle multiplicity $({\rm d}N_\gamma/{\rm d}y = A \times ({\rm d}N_{\rm ch}/{\rm d}\eta)^\alpha)$ and the scaling factor $\alpha$ is about 1.25 for yields in heavy-ion collisions at $\sqrt{s_{NN}} = 39$–200 GeV. The scaling factors in small systems, $p$+Au and $d$+Au collisions, are located in between $p+p$ and heavy-ion results. A new analysis has been performed with enhanced statistics of Au+Au data [8, 9]. The left panel of Fig. 5 shows the scaling factor $\alpha$ as a function of direct photon $p_{\rm T}$ in the integrated centrality of Au+Au collisions. Interestingly, the scaling factor weakly depends on $p_{\rm T}$, although the source of direct photons varies with $p_{\rm T}$. When comparing with direct photon yields at 2.76 TeV [10], good scaling with multiplicity is observed for $p_{\rm T} < 2$ GeV$/c$ from 39 GeV to 2.76 TeV. At $p_{\rm T} > 2$ GeV$/c$, the yield at 2.76 TeV is larger than the scaled yield based on the RHIC energies. This indicates that the medium temperature is higher at the LHC energy.

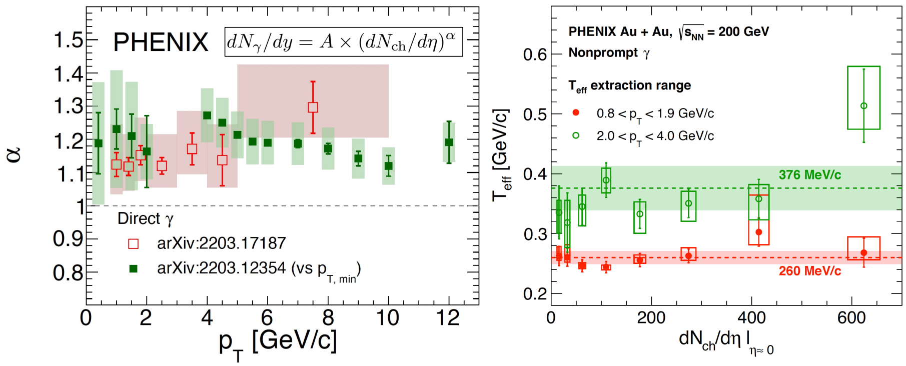


Fig. 5. Scaling factors $\alpha$ as a function of direct photon $p_{\mathrm{T}}$ and inverse slope parameters from non-prompt photon $p_{\mathrm{T}}$ spectra as a function of charged particle multiplicity in two $p_{\mathrm{T}}$ ranges.

For more investigation on the sources of direct photons at low $p_{\mathrm{T}}$, the non-prompt direct photon yields are calculated by subtracting the scaled $p+p$ yield [9]. The $p_{\mathrm{T}}$ spectra of non-prompt direct photons are not described by a single exponential function ($\exp(-p_{\mathrm{T}}/T_{\mathrm{eff}})$), so the inverse slope parameters are extracted at two $p_{\mathrm{T}}$ ranges, $0.8 < p_{\mathrm{T}} < 1.9$ GeV/$c$ and $2 < p_{\mathrm{T}} < 4$ GeV/$c$, for each non-prompt direct photon $p_{\mathrm{T}}$ spectrum. The right panel of Fig. 5 shows the inverse slope parameter as a function of multiplicity. A higher value is obtained at the higher-$p_{\mathrm{T}}$ range, indicating that the non-prompt direct photons in different $p_{\mathrm{T}}$ are produced at different stages, and there is no significant multiplicity dependence.

### *2.2. $\pi^0$–$h$ correlation*

The modification of jet shape inside the QGP can be studied via the azimuthal correlation between trigger particles at high $p_{\mathrm{T}}$ and associated particles in various $p_{\mathrm{T}}$ ranges. New preliminary results on $\pi^0$–$h$ correlations have been obtained with high statistics data collected in 2014. Figure 6 shows per-trigger yields as a function of $\Delta\phi$ of $\pi^0$–$h$ correlation in the $p+p$ and central Au+Au collisions. The trigger particles in $4 < p_{\mathrm{T}} < 5$ GeV/$c$, and associated particles in two $p_{\mathrm{T}}$ ranges, $0.5 < p_{\mathrm{T}} < 1$ GeV/$c$ (left) and $3 < p_{\mathrm{T}} < 5$ GeV/$c$ (right), are shown. The bottom panels show the difference in the per-trigger yields between the two systems. In the results for low-$p_{\mathrm{T}}$ associated particles, the yields in Au+Au are larger than those in $p+p$ at the broad $\Delta\phi$ range. However, the yield in Au+Au is smaller at $\Delta\phi \sim \pi$ for associated particles in the higher-$p_{\mathrm{T}}$ region. The results suggest a picture that high-$p_{\mathrm{T}}$ partons around the core of jets lose energy, and the energy is redistributed broadly to low-$p_{\mathrm{T}}$ partons.

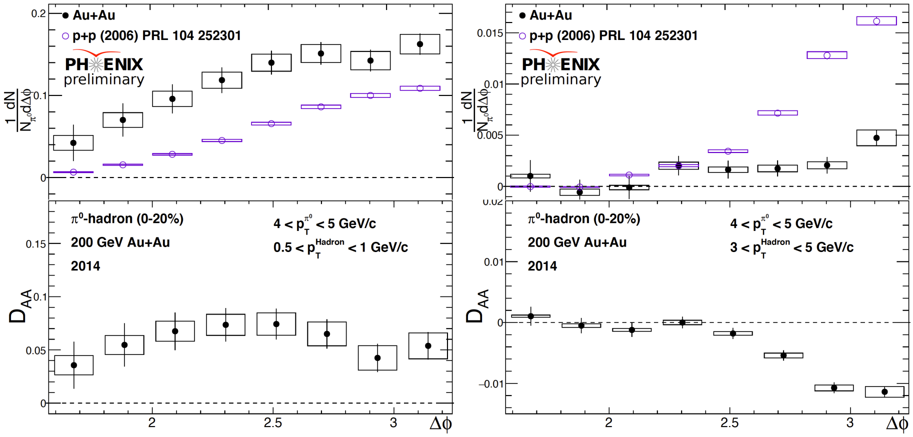


Fig. 6. The per-trigger pair yields of $\pi^0$–$h$ correlation in the $p+p$ and central Au+Au collisions at $\sqrt{s_{NN}} = 200$ GeV for two $p_T$ ranges of associated particles and the difference between results in two systems.

### *2.3. Electrons from charm and bottom decay*

Heavy quarks are useful tools to investigate the medium properties of the QGP. The modifications of charm and bottom quarks are expected to be different, and one possible reason is the dead-cone effect. PHENIX has measured yields of electrons from charm- and bottom-hadron decays both in the $p+p$ and Au+Au collisions at $\sqrt{s_{NN}} = 200$ GeV [11, 12], and the nuclear modification factor ($R_{AA}$) is calculated with the yields obtained using the same analysis method. Figure 7 shows $R_{AA}$ of electrons from charm- (black/green curves) and bottom- (gray/blue curves) hadron decays in the peripheral (left) and central (right) Au+Au collisions $\sqrt{s_{NN}} = 200$ GeV, and the ratio of bottom electron $R_{AA}$ to charm electron $R_{AA}$ is presented in the bottom panels. In the peripheral collisions, the nuclear modification factor for charm and bottom electrons is consistent within the uncertainties. However, the modification is more substantial for charm electrons than bottom electrons in the central collisions indicating quark mass-dependent energy loss inside the QGP.

### *2.4. J/ψ elliptic flow*

In early studies of $J/\psi$ production and its modification in heavy-ion collisions at RHIC and LHC energies, it was found that the regeneration effect is important at the LHC energy but may not at the RHIC energy [13, 14]. In addition to the nuclear modification factor, elliptic flow ($v_2$) can provide more information on mechanisms of the $J/\psi$ production in heavy-ion collisions. PHENIX has measured $J/\psi$ $v_2$ at forward rapidity in 10–60%

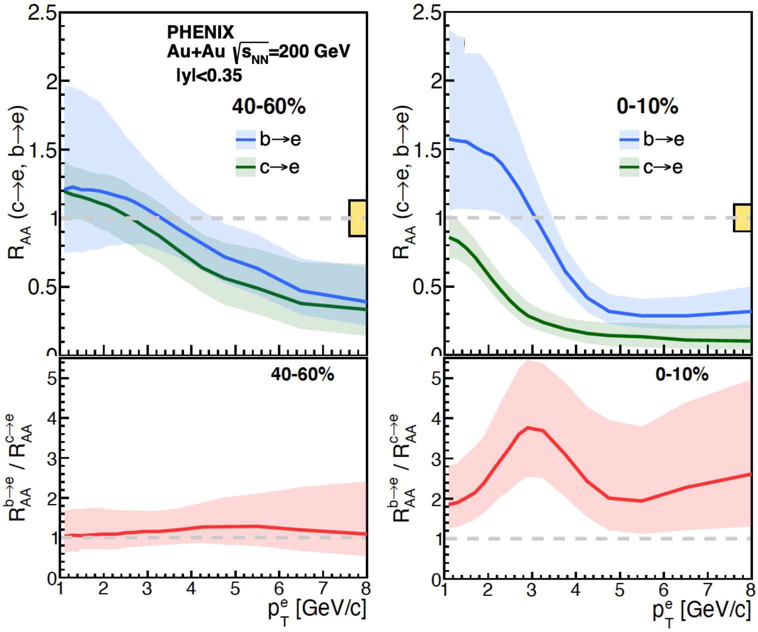


Fig. 7. (Color online) Nuclear modification factor of electrons from charm and bottom hadron decays in peripheral (left) and central (right) Au+Au collisions at $\sqrt{s_{NN}} = 200$ GeV. The ratio of electron $R_{AA}$ from bottom hadron to charm hadron is presented in the bottom panels.

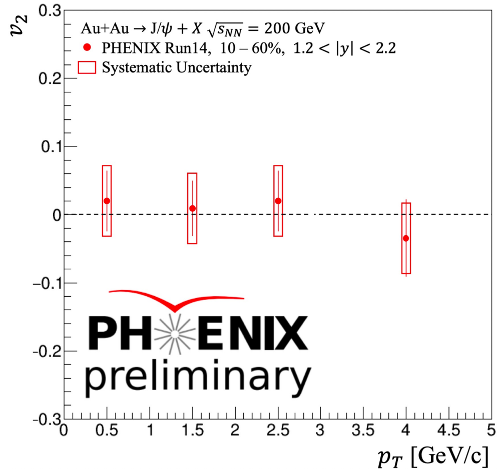


Fig. 8. Elliptic flow of $J/\psi$ as a function of $p_{\mathrm{T}}$ at forward rapidity in 10–60% Au+Au collisions at $\sqrt{s_{NN}} = 200$ GeV.

Au+Au collisions at $\sqrt{s_{NN}} = 200$ GeV as presented in Fig. 8, and it is consistent with zero within uncertainties. The PHENIX results are different from the non-zero $v_2$ results at the LHC energies [15], and this indicates that the regeneration effect is small at forward rapidity at the RHIC energies.

## 3. Summary and outlook

In summary, PHENIX has obtained results indicating QGP droplets in small systems such as collectivity, nuclear modification of light-flavor hadrons, and $\psi(2S)$ in high multiplicity events. In large systems, detailed studies of the QGP have been done with direct photons, particle correlations, heavy-flavor electrons, and quarkonia. PHENIX recently completed the data production of all collected data, so the full statistics of Au+Au data collected in 2014 and 2016 are ready for analysis in the future.

## REFERENCES


[1] PHENIX Collaboration, *Nat. Phys.* **15**, 214 (2019).

[2] PHENIX Collaboration (U.A. Acharya *et al.*), *Phys. Rev. C* **105**, 024901 (2022).

[3] PHENIX Collaboration (U.A. Acharya *et al.*), `arXiv:2203.09894 [nucl-ex]`.

[4] PHENIX Collaboration (U.A. Acharya *et al.*), *Phys. Rev. C* **105**, 064902 (2022).

[5] PHENIX Collaboration (U. Acharya *et al.*), *Phys. Rev. C* **106**, 014908 (2022), `arXiv:2203.06087 [nucl-ex]`.

[6] PHENIX Collaboration (U. Acharya *et al.*), *Phys. Rev. C* **102**, 014902 (2020).

[7] PHENIX Collaboration (U.A. Acharya *et al.*), *Phys. Rev. C* **105**, 064912 (2022).

[8] PHENIX Collaboration (U.A. Acharya *et al.*), `arXiv:2203.12354 [nucl-ex]`.

[9] PHENIX Collaboration (U.A. Acharya *et al.*), `arXiv:2203.17187 [nucl-ex]`.

[10] ALICE Collaboration, *Phys. Lett. B* **754**, 235 (2016).

[11] PHENIX Collaboration (C. Aidala *et al.*), *Phys. Rev. D* **99**, 092003 (2019).

[12] PHENIX Collaboration (U.A. Acharya *et al.*), `arXiv:2203.17058 [nucl-ex]`.

[13] PHENIX Collaboration (A. Adare *et al.*), *Phys. Rev. C* **84**, 054912 (2011).

[14] ALICE Collaboration (B. Abelev *et al.*), *Phys. Rev. Lett.* **109**, 072301 (2012).

[15] ALICE Collaboration (S. Acharya *et al.*), *J. High Energy Phys.* **2019**, 012 (2019).